Matrix Isolation

DOI: 10.1002/ange.200502503

Experimental Evidence for a Jahn–Teller Distortion in $AuCl_3$**

*Ian J. Blackmore, Adam J. Bridgeman, Neil Harris, Mark A. Holdaway, John F. Rooms, Emma L. Thompson, and Nigel A. Young**

Gold halides have generated considerable interest amongst both computational and experimental chemists because of their intriguing bonding and structures.[1–4] Advances in gas-phase (mass-spectrometry) experiments[5] and the theoretical importance of relativistic effects in gold chemistry[6] have recently been reviewed. The common oxidation states for gold are Au^{III} and Au^{I}, with Au^{II} being comparatively rare. The Au^{I} monohalides display large structural relativistic effects, and the very short Au···Au distances in their dimers (caused by the so-called "aurophilic attraction") are regarded as classic examples of metallophilic interactions.[6] All of the monohalides have been characterized experimentally.[1,5,7] Monomeric Au^{II} is a rare oxidation state, although multinuclear complexes are more common,[8] and some examples such as solid-state $AuCl_2$ are mixed valent.[9] Perhaps the most significant Au^{II} complexes are those containing Au–Xe bonds, such as $[AuXe_4][Sb_2F_{11}]_2$.[10] Schröder et al. have recently identified $AuCl_2$ (as neutral, anionic, and cationic species) in sophisticated mass-spectrometric experiments.[11] The D_{3h} trigonal-planar structure of the d^8 Au^{III} halides are Jahn–Teller distorted to T-, Y-, and L-shaped geometries. This distortion was highlighted computationally by Schwerdtfeger et al. in 1992,[12] and recently elaborated by Hargittai and co-workers[1–3] as well as by Schwerdtfeger and co-workers.[4] Both the stability of the gold trihalides and the Jahn–Teller stabilization energy decrease from the fluoride through to the iodide. The T-shaped structure is the minimum of the Jahn–Teller surface for AuF_3, $AuCl_3$, and $AuBr_3$, and is the global minimum of the ground state for the first two. The Y-shaped geometry is a transition state between the T-shaped geometries. For AuI_3, the Y-shaped structure lies at lower energy than the T-shaped structure, but for both $AuBr_3$ and AuI_3 the potential-energy surface is very flat, and the energy gain arising from a Jahn–Teller distortion is small. Schulz and Hargittai[1] suggest that AuF_3 and $AuCl_3$ are static Jahn–Teller

[*] I. J. Blackmore, Dr. A. J. Bridgeman, Dr. N. Harris, M. A. Holdaway, Dr. J. F. Rooms, Dr. E. L. Thompson, Dr. N. A. Young
Department of Chemistry
The University of Hull
Kingston upon Hull, HU6 7RX (UK)
Fax: (+44) 1482-466-410
E-mail: n.a.young@hull.ac.uk

[**] This work was supported by the Engineering and Physical Sciences Research Council UK (EPSRC-GR/T09651) and the University of Hull.

Supporting information for this article is available on the WWW under http://www.angewandte.org or from the author.

systems, whereas $AuBr_3$ and AuI_3 are dynamic Jahn–Teller systems. Of the monomeric Au^{III} halides, experimental data is only available for AuF_3, with the T-shaped structure being confirmed by electron diffraction studies.[13] AuI_3 has been reported to be stabilized in a cuprate lattice,[14] but more recent calculations[15] and experiments[16] suggest that the gold is present as Au^{I} and not Au^{III}, therefore the D_{3h} structure is unsurprising. The solid-state structures of both Au_2Cl_6 and Au_2Br_6 consist of discrete D_{2h}-symmetric halogen-bridged dimers[12] which become the principal gold-containing vapor species. Vaporization is accompanied by extensive decomposition, and in the recent electron-diffraction study, only approximately 6% of the vapor was Au_2Cl_6 (the remainder being Cl_2), and it was noted that it was not possible to obtain any data for monomeric $AuCl_3$.[2] Therefore, the authors proposed that the only way forward was to use detailed computational methods.

We have previously used matrix isolation in combination with IR, UV/Vis and extended X-ray absorption fine structure (EXAFS) spectroscopy to synthesize and characterize monomeric noble-metal chlorides such as PtCl and $PtCl_2$.[17] For the platinum chlorides, hollow-cathode sputtering with chlorine-doped argon was used to generate the atomic Pt, and although this approach was used for $AuCl_3$, thermal evaporation and laser ablation were also employed.

Figure 1a shows the electronic absorption spectrum of Au_2Cl_6 in an argon matrix, and is in good agreement with the vapor-phase spectrum.[18] The intense bands at 40590 and 46060 cm^{-1} were assigned to bridging- and terminal-ligand-to-metal charge-transfer transitions, respectively.[18] The weaker features at 22300 and 32890 cm^{-1} were assigned to d-d transitions.[18] Figure 1b shows the spectrum obtained when thermally evaporated gold atoms were matrix isolated in 1% Cl_2/Ar. The sharp peaks at 39050, 43670, and 44085 cm^{-1} are due to atomic gold.[19] The broad feature at approximately 30500 cm^{-1} and the tail into the UV region are both due to Cl_2. In addition to these, a weaker band at about 16000 cm^{-1} with vibrational fine structure was observed. The spectra obtained when thermally evaporated gold atoms were trapped in a 5% Cl_2/Ar matrix were very similar, except that there was less unreacted gold, and the fine structure on the band at 16000 cm^{-1} was less well resolved. A similar spectrum was obtained when gold was sputtered with Cl_2/Ar mixtures, and the band at 16000 cm^{-1} was also present when HCl was used as the chlorine source in the sputtering experiments. Figure 1c shows the spectrum obtained when thermally evaporated gold atoms were condensed in a 1% Cl_2/Ar mixture that had passed through a microwave discharge just prior to deposition. This process had the effect of increasing the yield of the feature at 16000 cm^{-1} relative to similar experiments with no discharge, as well as reducing the amount of residual Cl_2 present, although there is a substantial amount of unreacted gold. These observations indicate that the band at 16000 cm^{-1} only appears when chlorine atoms or molecules are present, and that there are no high energy features associated with the band at 16000 cm^{-1} that are obscured by the UV tail arising from the presence of Cl_2 (Figure 1b). As the feature at 16000 cm^{-1} was only present in spectra which contained both gold and chlorine and is independent of the source of both gold atoms and chlorine, it can readily be assigned to an $AuCl_x$ species. An expansion of the vibrational fine structure on this band is shown in Figure 1d, and the separation of about 310 cm^{-1} between the sharpest peaks on the low energy side is consistent with a symmetric Au–Cl stretching mode in an excited state. The observation of only one band implies the presence of one $AuCl_x$ species. As this band is much lower in energy than both the charge-transfer and d-d bands in Au_2Cl_6, it is most likely to be a d-d transition, with any charge-transfer bands beyond the effective upper spectral limit of about 50000 cm^{-1}.

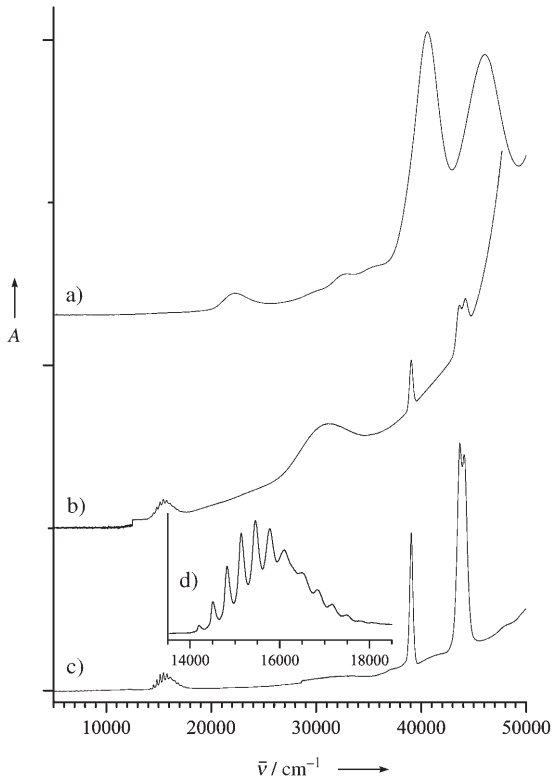

Figure 1. Matrix-isolation electronic absorption spectra of a) Au_2Cl_6 in Ar, b) thermally evaporated gold atoms in 1% Cl_2/Ar, c) thermally evaporated gold atoms mixed with 1% Cl_2/Ar passed through microwave discharge, d) expansion of (c).

IR spectroscopy of the Au–Cl stretching modes (ν_{Au-Cl}) in combination with the natural isotopic abundances of Cl (^{35}Cl, 75.5%; ^{37}Cl, 24.5%) is a very powerful method of identifying molecular shape. For AuCl, a simple 3:1 isotope pattern is expected. For $AuCl_2$, a 9:6:1 pattern would be observed, and if the separation of the outermost components could be identified accurately, the bond angle could be determined. The presence of threefold rotation axes in both D_{3h}- and C_{3v}-symmetric $AuCl_3$ would result in nonbinomial isotope patterns for the degenerate modes. One IR-active E′ ν_{Au-Cl} band with a 81:9:27:11 pattern is expected for D_{3h}-symmetric $AuCl_3$, whereas C_{3v}-symmetric $AuCl_3$ would have two IR-active ν_{Au-Cl} bands, an E mode with a 81:9:27:11 isotope pattern, and an A_1 mode with a 27:27:9:1 pattern. Calculations[1,2] for T-shaped $AuCl_3$ predict three IR-active ν_{Au-Cl} modes ($2A_1 + B_2$), but the two A_1 modes have very low intensity so that only the B_2 mode is expected to be observed.

Our calculations indicate that the B_2 mode will display a 9:6:1 chlorine isotope pattern, and the two very low intensity A_1 modes will yield a complex isotope pattern derived from 9:6:1 and 3:1 isotope patterns, but which is dependent on their separation. The Y-shaped transition state is also calculated[1,2] to have three IR-active ν_{Au-Cl} modes ($2A_1 + B_2$) with similar frequency, intensity (intense A_1, very weak $A_1 + B_2$), and isotope patterns to the T-shaped geometry.

The argon-matrix IR spectrum of Au_2Cl_6 is shown in Figure 2a. This spectrum is in very good agreement with the previous data from both the solid state and the gas phase,[20] and complex chlorine isotopic structure is observed in both bands. The feature at approximately 386 cm^{-1} arises from terminal ν_{Au-Cl} asymmetric stretching modes ($\nu_{12}(B_{2u})$ and $\nu_{16}(B_{3u})$), and the bridging ν_{Au-Cl} asymmetric stretching modes are at about 312 cm^{-1} ($\nu_{13}(B_{2u})$ and $\nu_{17}(B_{3u})$). Figure 2b displays the spectrum of the matrix-isolated products from a gold foil sputtered with 5% Cl_2/Ar. The only significant ν_{Au-Cl} band is at approximately 420 cm^{-1}, and it is clear that there is no evidence for the formation of Au_2Cl_6 under these conditions. Although this band shows signs of asymmetry, it did not display isotopic chlorine features at higher spectral resolution, probably because of the considerable Cl_2 concentration in the matrix. Although sputtering, thermal evaporation, and laser ablation were all used with lower Cl_2/Ar concentrations, the spectral quality was not sufficient to provide convincing evidence of the geometry of the gold-containing species. Pure Cl_2 matrices were then used, and thermally evaporated gold atoms were condensed at 50 K and then cooled to about 12 K. The resulting spectrum is shown in Figure 2c. The most intense band at approximately 410 cm^{-1} clearly displays a 9:6:1 isotopic pattern with a splitting that is consistent with a vibrational mode involving two chlorine atoms attached to a heavy element. There is also evidence for a second 9:6:1 pattern with a similar peak separation a few wavenumbers higher. The most reasonable interpretation of this is that there are two 9:6:1 patterns in close proximity that are derived from the same vibrational mode, which is subject to matrix-site effects in the pure Cl_2 matrix. This band is in a very similar position to that obtained for argon matrices with sputtering, laser ablation, and thermal evaporation, thus indicating that it arises from the same species in all cases, which also gives rise to the band at 16000 cm^{-1} in the electronic absorption spectra. In addition to the relatively intense bands around 410 cm^{-1}, there is a complex multiplet at 375–350 cm^{-1}. Although $TaCl_5$ is known to have spectral features in this region,[21] no such bands were observed when a bare tantalum filament was heated during the deposition of a pure Cl_2 matrix. Therefore, this multiplet is also assigned to an $AuCl_x$ species.

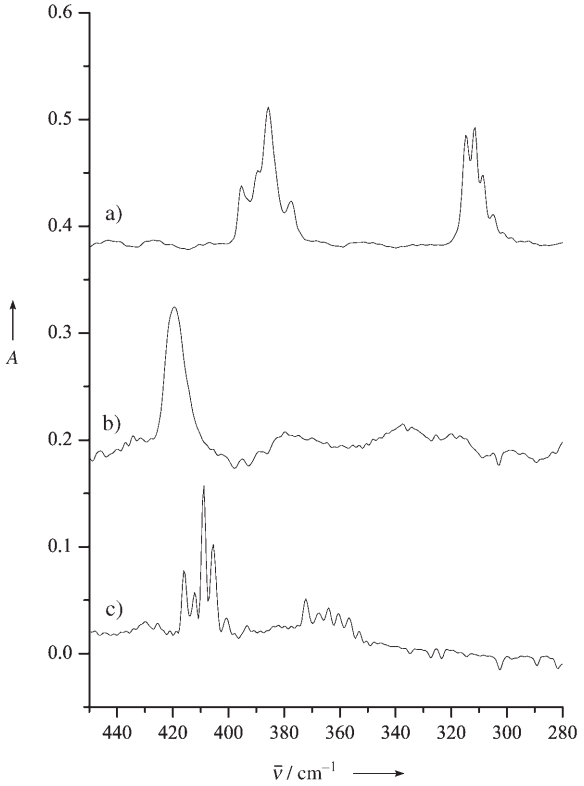

Figure 2. Matrix-isolation IR spectra of a) Au_2Cl_6 in Ar, b) gold atoms sputtered with 5% Cl_2/Ar, c) thermally evaporated gold atoms in 100% Cl_2.

The presence of 9:6:1 isotope patterns in the bands at 410 cm^{-1} rules out AuCl, but they could be assigned to either $AuCl_2$ or $AuCl_3$. Au^{II} is commonly considered to be a rare oxidation state, especially for monomeric compounds.[8] Solid-state $AuCl_2$ is known to be mixed valent[9] and $AuCl_2$ has only been detected in the vapor phase by using sophisticated mass spectrometric experiments starting with mass-selected $AuCl_2^-$.[11] Stace and co-workers have reported that Au^{II} can be stabilized in the gas phase by σ-donor, π-acceptor ligands, especially if the ligands have a large dipole moment and high ionization energy,[22] but this is not the case for chloride. It would be expected that pure Cl_2 matrices would yield stable gold chloride with the highest oxidation state. From all of the various experimental conditions used for the electronic absorption spectra, only one band at 16000 cm^{-1} was associated with both gold and chlorine, and whereas the presence of Cl atoms increased its intensity, no other bands were observed. The presence of weak features in the region between 375 and 350 cm^{-1} is compatible with $AuCl_3$, but not with $AuCl_2$. Despite reporting an extensive set of calculations on monomeric, dimeric, and anionic gold halides, Hargittai and co-workers[1,2] did not appear to consider $AuCl_2$. Schröder et al. have carried out some DFT calculations that indicate that $AuCl_2$ would be stable to disproportionation in the idealized gas phase, but not in the solid state.[11] Our DFT calculations[23] indicate that although the $\Delta_f H$ values for $AuCl_{2(g)}$ and $AuCl_{3(g)}$ from gold atoms and Cl_2 are very similar (−271 and −273 kJ mol^{-1}, respectively), the enthalpy of atomization to gold and chlorine atoms is much larger for $AuCl_3$ than for $AuCl_2$ (672 and 537 kJ mol^{-1}, respectively). The previous MP2 and B3LYP calculations[2] indicate that the IR-active ν_{Au-Cl} mode of "T-shaped" $AuCl_3$ should be about 20 cm^{-1} higher than the terminal ν_{Au-Cl} modes in Au_2Cl_6, with the most intense ν_{Au-Cl} mode of the Y-shaped transition state being a few wavenumbers less than that of the T-shaped ν_{Au-Cl}

mode. The ν_{Au-Cl} mode of AuCl is calculated[2] to be just above midway in terms of energy between the terminal and bridging ν_{Au-Cl} modes in Au_2Cl_6, although our DFT calculations incorporating the high-level relativistic effects within ADF (Amsterdam Density Functional package) indicate that the value should be closer to that of the terminal ν_{Au-Cl} mode in Au_2Cl_6. Our calculations on $AuCl_2$ indicate that its IR-active ν_{Au-Cl} mode should be higher than that of $AuCl_3$ by about 17 cm^{-1}.

Therefore, on the basis of both experimental and computational considerations, the most reasonable assignment of the bands at about 420 cm^{-1} in the IR spectrum is to $AuCl_3$. The 9:6:1 chlorine isotope pattern demonstrates that it does not have D_{3h} (or C_{3v}) symmetry but adopts a Jahn–Teller-distorted geometry, which on the basis of the calculations[2] is most likely to be T shaped. These calculations also indicate that the two A_1 modes in the T-shaped $AuCl_3$ species will be separated by about 10 cm^{-1} and be about 30 cm^{-1} lower than the B_2 mode, but will have very low (effectively zero) intensity. The two low-intensity A_1 and B_2 modes in the Y-shaped geometry are also calculated to be separated by 10 cm^{-1}, and about 30–40 cm^{-1} lower than the intense A_1 mode. The complex multiplet at 375–350 cm^{-1} clearly falls into this region, but the intensity is incompatible with the calculations.[2] It is possible that the Cl_2 matrix exerts sufficient perturbation so that these modes gain some intensity. The isotope pattern is very sensitive to the separation of the two modes, and as a site effect was observed on the intense ν_{Au-Cl} mode, it is likely that this multiplet is also subject to site effects.

The Au L_3-edge EXAFS and FT for the matrix products of gold sputtered with 5% Cl_2/Ar are shown in Figure 3. Sputtering was chosen as it gives the best dilution of metal atoms in the matrix, thus avoiding the problems of aggregation.[17] The FT contains one peak that fits[24] to a single Au–Cl bond length with no evidence for two different bond lengths, thus ruling out the presence of Au_2Cl_6. The Au–Cl bond length of 2.22(2) Å is 0.06 Å shorter than that observed for $[AuCl_4]^-$ with the same analysis protocols. Previous B3LYP and MP2 calculations[2] indicate that the T-shaped ground state of $AuCl_3$ will have Au–Cl bond lengths shorter by about 0.07 Å than $[AuCl_4]^-$, and our ADF calculations indicate that the Au–Cl bond length in $AuCl_2$ will be approximately 0.04 Å shorter than that of $AuCl_3$. The chlorine occupation number refined to a value of about 1.7, or an $AuCl_3$ fraction of about 57%. Whereas this could indicate a lower-coordination species, the presence of bands corresponding to unreacted gold in all of the electronic absorption spectra, the IR evidence for $AuCl_3$, as well as the Au–Cl bond lengths, indicate it is much more likely to be caused by the presence of both $AuCl_3$ and Au in the matrix. Although the small peak at around 4.4 Å in the FT might be due to multiple scattering pathways through the central Au atom, indicative of a linear or very near linear (>160°) $AuCl_2$ unit,[25] its intensity is too low to make any firm conclusions, and this is also where Au···Ar interactions would be expected.

In conclusion a combination of matrix-isolation electronic absorption, IR, and Au L_3-edge EXAFS has provided the first experimental data for $AuCl_3$ and shown conclusively that it does not have D_{3h} symmetry in the matrix, but rather a Jahn–Teller-distorted geometry. The experimental data is consistent with a calculated ground state having a T-shaped geometry.

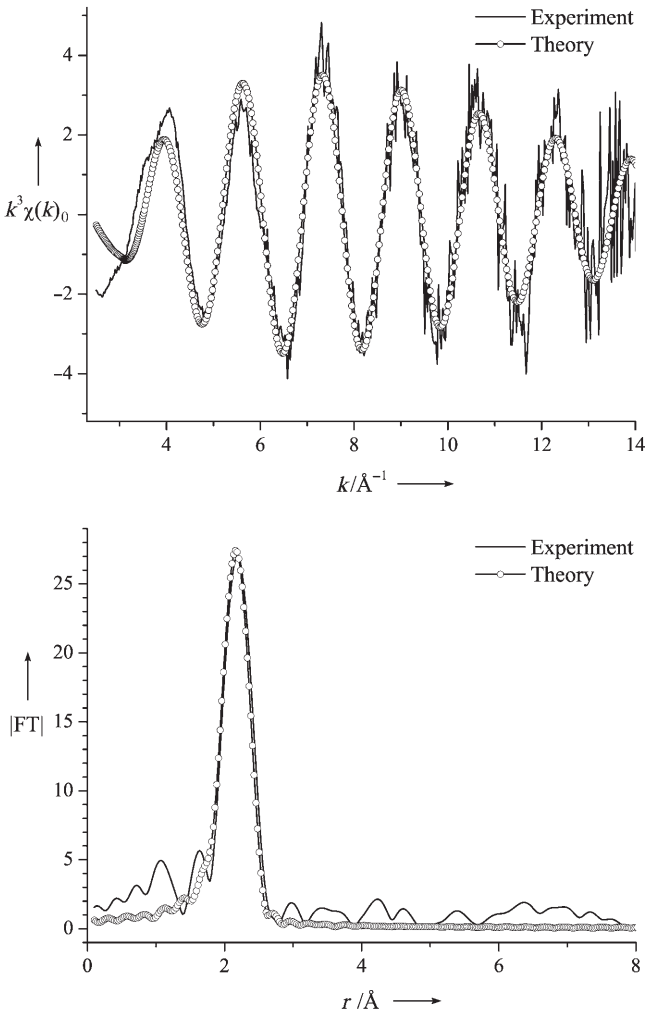

Figure 3. Au L_3-edge EXAFS (top) and FT (bottom) of the matrix-isolated products of gold atoms sputtered with 5% Cl_2/Ar.

Experimental Section

The general features of our matrix-isolation experimental methodology have been described previously.[17] The gold atoms were sputtered from a gold-foil hollow cathode, thermally evaporated from gold wire wound onto a tungsten filament, or laser ablated (Xe–Cl excimer laser) from a gold target disc. The Cl_2/Ar mixtures were prepared by using standard manometric procedures. The Au L_3-edge EXAFS spectra were collected on station 9.2 of the Daresbury Laboratory SRS (2 GeV, 150–250 mA) using a Si220 monochromator detuned by 50% to reduce harmonic contamination. The fluorescence data were collected with a Canberra 13-element solid-state detector. The spectra were averaged, calibrated (using the first maximum in the first derivative of gold foil at 11919 eV), and background subtracted (quadratic pre-edge, 6th-order polynomial post-edge) by using PAXAS.[26] The data were modeled with EXCURV98.[27] The DFT calculations at 0 K with zero-point energy

and basis-set supposition-error corrections used ADF BP86/TZP with ZORA.[28]

Received: July 18, 2005
Published online: September 27, 2005

Keywords: density functional calculations · EXAFS spectroscopy · gold · Jahn–Teller distortion · matrix isolation

[1] A. Schulz, M. Hargittai, *Chem. Eur. J.* **2001**, *7*, 3657.
[2] M. Hargittai, A. Schulz, B. Réffy, M. Kolonits, *J. Am. Chem. Soc.* **2001**, *123*, 1449.
[3] B. Réffy, M. Kolonits, A. Schulz, T. M. Klapötke, M. Hargittai, *J. Am. Chem. Soc.* **2000**, *122*, 3127.
[4] T. Sohnel, R. Brown, L. Kloo, P. Schwerdtfeger, *Chem. Eur. J.* **2001**, *7*, 3167.
[5] H. Schwarz, *Angew. Chem.* **2003**, *115*, 4580; *Angew. Chem. Int. Ed.* **2003**, *42*, 4442.
[6] P. Pyykkö, *Angew. Chem.* **2004**, *116*, 4512; *Angew. Chem. Int. Ed.* **2004**, *43*, 4412.
[7] D. Schröder, J. Hrusák, I. C. Tornieporth-Oetting, T. M. Klapötke, H. Schwarz, *Angew. Chem.* **1994**, *106*, 223; *Angew. Chem. Int. Ed. Engl.* **1994**, *33*, 212.
[8] A. Laguna, M. Laguna, *Coord. Chem. Rev.* **1999**, *195*, 837.
[9] D. B. Dell'Amico, F. Calderazzo, F. Marchetti, *J. Chem. Soc. Dalton Trans.* **1976**, 1829; D. B. Dell'Amico, F. Calderazzo, F. Marchetti, S. Merlino, G. Perego, *J. Chem. Soc. Chem. Commun.* **1977**, 31.
[10] S. Seidel, K. Seppelt, *Science* **2000**, *290*, 117; T. Drews, S. Seidel, K. Seppelt, *Angew. Chem.* **2002**, *114*, 470; *Angew. Chem. Int. Ed.* **2002**, *41*, 454; K. Seppelt, *Z. Anorg. Allg. Chem.* **2003**, *629*, 2427.
[11] D. Schröder, R. Brown, P. Schwerdtfeger, X. B. Wang, X. Yang, L. S. Wang, H. Schwarz, *Angew. Chem.* **2003**, *115*, 323; *Angew. Chem. Int. Ed.* **2003**, *42*, 311.
[12] P. Schwerdtfeger, P. D. W. Boyd, S. Brienne, A. K. Burrell, *Inorg. Chem.* **1992**, *31*, 3411.
[13] B. Réffy, M. Kolonits, A. Schulz, T. M. Klapötke, M. Hargittai, *J. Am. Chem. Soc.* **2001**, *123*, 1545.
[14] J. H. Choy, Y. I. Kim, S. J. Hwang, P. V. Huong, *J. Phys. Chem. B* **2000**, *104*, 7273.
[15] M. L. Munzarova, R. Hoffmann, *J. Am. Chem. Soc.* **2002**, *124*, 5542.
[16] J. H. Choy, Y. I. Kim, *J. Phys. Chem. B* **2003**, *107*, 3348.
[17] A. J. Bridgeman, G. Cavigliasso, N. Harris, N. A. Young, *Chem. Phys. Lett.* **2002**, *351*, 319.
[18] D. S. Rustad, N. W. Gregory, *Polyhedron* **1991**, *10*, 633; L. Nalbandian, S. Boghosian, G. N. Papatheodorou, *Inorg. Chem.* **1992**, *31*, 1769.
[19] D. M. Gruen, S. L. Gaudioso, R. L. McBeth, J. L. Lerner, *J. Chem. Phys.* **1974**, *60*, 89; D. M. Gruen, J. K. Bates, *Inorg. Chem.* **1977**, *16*, 2450.
[20] L. Nalbandian, G. N. Papatheodorou, *Vib. Spectrosc.* **1992**, *4*, 25.
[21] R. K. Bellingham, J. T. Graham, P. J. Jones, J. R. Kirby, W. Levason, J. S. Ogden, A. K. Brisdon, E. G. Hope, *J. Chem. Soc. Dalton Trans.* **1991**, 3387.
[22] N. R. Walker, R. R. Wright, P. E. Barran, J. N. Murrell, A. J. Stace, *J. Am. Chem. Soc.* **2001**, *123*, 4223; N. R. Walker, R. R. Wright, P. E. Barran, A. J. Stace, *Organometallics* **1999**, *18*, 3569.
[23] The $\Delta_f H$ values for $AuCl_{(g)}$, $AuCl_{2(g)}$, and $AuCl_{3(g)}$ from $Au_{(g)}$ and $Cl_{2(g)}$ are -147, -271, and $-273\,kJ\,mol^{-1}$, respectively. The $\Delta_{atm} H$ values for $AuCl_{(g)}$, $AuCl_{2(g)}$, and $AuCl_{3(g)}$ are $+280$, $+537$, and $+672\,kJ\,mol^{-1}$, respectively.
[24] Refined Au L_3-edge EXAFS parameters. $AuCl_3$ (r_{Au-Cl}, 2.224(5) Å; $2\sigma^2$, 0.007(1); E_f, −8.1(12), R, 41.1 %). $H[AuCl_4]\cdot 3H_2O$ (r_{Au-Cl}, 2.282(2) Å; $2\sigma^2$, 0.006(1); E_f, −11.7(4), R, 19 %). The literature r_{Au-Cl} values for $H[AuCl_4]\cdot 4H_2O$ are 2.283 and 2.286 Å (J. M. Williams, S. W. Peterson, *J. Am. Chem. Soc.* **1969**, *91*, 776).
[25] A. van der Gaauw, O. M. Wilkin, N. A. Young, *J. Chem. Soc. Dalton Trans.* **1999**, 2405.
[26] N. Binsted, *PAXAS, Program for the analysis of X-ray absorption spectra*, University of Southampton, UK, **1988**.
[27] N. Binsted, *EXCURV98, CCLRC Daresbury Laboratory Computer Program*, CCLRC, Daresbury Laboratory, UK, **1998**.
[28] C. Fonseca Guerra, J. G. Snijders, G. te Velde, E. J. Baerends, *Theor. Chem. Acc.* **1998**, *99*, 391; G. te Velde, F. M. Bickelhaupt, E. J. Baerends, C. Fonseca Guerra, S. J. A. van Gisbergen, J. G. Snijders, T. Ziegler, *J. Comput. Chem.* **2001**, *22*, 931; *ADF2002.02*, SCM, Theoretical Chemistry, Vrije Universiteit, Amsterdam, **2002**.

